Pictorial Essay

Spectrum of brain abnormalities detected on whole body F-18 FDG PET/CT in patients undergoing evaluation for non-CNS malignancies

Madhavi Tripathi, Abhinav Jaimini, Maria M D'Souza, Rajnish Sharma, Jyotika Jain[1], Gunjan Garg, Dinesh Singh, Nitin Kumar[2], Anil K Mishra[2], Rajesh K Grover[1], Anupam Mondal

Division of PET Imaging, Molecular Imaging and Research Centre, [2]Division of Cyclotron and Radiopharmaceutical Sciences, MIRC, Institute of Nuclear Medicine and Allied Sciences, Lucknow Road, Delhi, [1]Delhi State Cancer Institute, GTB Hospital, Shahdara, Delhi, India

ABSTRACT

We present the pattern of metabolic brain abnormalities detected in patients undergoing whole body (WB) F-18 flurodeoxyglucose (FDG) positron emission tomography/computed tomography (PET/CT) examination for non-central nervous system (CNS) malignancies. Knowledge of the PET/CT appearance of various intracranial metabolic abnormalities enables correct interpretation of PET scans in oncological patients where differentiation of metastasis from benign intracranial pathologies is important and improves specificity of the PET study. A complete clinical history and correlation with CT and MRI greatly helps in arriving at a correct imaging diagnosis.

Keywords: Arachnoid cyst, brain metastases, F-18 FDG, PET/CT, infarct

INTRODUCTION

We present a compilation of cases representing the spectrum of incidentally detected metabolic brain abnormalities in patients undergoing whole body (WB) F-18 flurodeoxyglucose (FDG) positron emission tomography/computed tomography (PET/CT) examination for non-central nervous system (CNS) oncological indications.

The PET/CT study was performed on a Discovery STE 16 (GE) camera which combines a helical 16 slice CT with a BGO block tomography. This has a transaxial resolution FWHM for 3D mode at 1cm offset from the centre of field of view of 5.12mm. Whole body PET scans at our institution includes images from the vertex to mid-thigh that are obtained 60 minutes following intravenous tracer injection of 370 MBq of F-18 FDG. An initial scout from vertex to mid-thigh for localizer positioning is followed by the low dose non-contrast CT (NCCT) acquisition at 120 KVn and 110 mA for attenuation correction and anatomical coregistration. This is followed by a 2 minute per bed position 3D emission PET scan which includes the brain and is completed in six or seven bed positions depending on patient height. Wherever considered necessary a separate PET/CT scan of the brain is acquired for 8 minutes single bed position. Data is reconstructed using 3D VUE algorithm (GE) and images are viewed for interpretation on a Xeleris workstation using Volumetrix protocol (GE). First the maximum intensity projection (MIP) image is viewed in cine mode with window variation for lesion localization in the entire imaged field including the brain. This is followed by setting the plain PET window and simultaneous viewing of plain PET and fused PET/CT images for localization of lesion from eye to thigh. Next, the CT window is adjusted for brain visualization and PET window was adjusted for grey matter white matter distinction. Plain PET and fused PET/CT images are then analyzed visually for abnormal tracer localization and corresponding CT abnormality.

Access this article online

Quick Response Code:

Website: www.ijnm.in

DOI: 10.4103/0972-3919.90271

Intracranial metabolic abnormalities localized on the F-18 FDG PET/CT study were:

Brain metastases

F-18 FDG-PET/CT is being used to evaluate patients with a variety of malignancies because in a single imaging session it

Address for correspondence:
Dr. Madhavi Tripathi, Division of PET Imaging, Molecular Imaging and Research Centre, Institute of Nuclear Medicine and Allied Sciences, Timarpur, Delhi-110 054, India. E-mail: madhu_deven@yahoo.com

provides useful information about disease stage and can help in identification of sites of metastatic disease not detected by using other imaging techniques. Accurate identification of cerebral metastases (mets) is important for staging, prognosis and determination of appropriate therapy.[1-3] The incidence of spread of systemic cancer to the brain ranges from 20% to 40%, depending on whether surgical, radiologic or autopsy data are reviewed. In a large series reviewing sources of brain metastases, the primary tumors in descending frequency comprise lung, breast, malignant melanoma, renal cell, gastrointestinal tract, uterine and carcinomas of unknown primary.[4] On FDG-PET there could be several patterns of cerebral metastasis, varying from a solitary [Figure 1] to multiple in number [Figure 2], hyper-metabolic (increased FDG uptake) or hypo-metabolic (reduced FDG uptake) [Figure 3] lesions corresponding to iso or hyper-dense lesions with or without associated edema on NCCT [Table 1]. In our experience, hyper-metabolic brain mets show good contrast resolution and can be appreciated on the MIP image itself [Figure 2a, b]. Hypo-metabolic mets on the other hand are poorly appreciated on the MIP image unless associated with surrounding edema which causes appreciable hypometabolism. Small hypo-metabolic mets could easily be overlooked [Figure 3d] on PET/NCCT images though contrast enhanced CT (CECT) [Figure 3e] clearly highlights these lesions. In these patients, though the primary lesions are FDG avid, the reason for the cerebral mets being hypo-metabolic remains enigmatic. Cystic and necrotic cerebral mets may also be hypo-metabolic.[5] Primaries where cerebral metastases are rare and if asymptomatic can also be detected on the WB FDG PET study. Like in a treated case of carcinoma ovary with rising Ca-125 levels post-therapy [Figure 4], the only lesion detected was a solitary brain metastases on FDG PET/CT which was subsequently resected. Conventionally it would have been quite difficult in this asymptomatic patient to think of a brain metastases as the cause of rising Ca-125. The role of brain imaging with PET in patients undergoing staging of non-CNS malignancies has been questioned and previous studies have shown that PET performed inferior to other modalities.[1,6-9] In a review of 20 patients with cerebral metastases identified by CT or MRI, only 68% of the lesions were detected on FDG-PET.[9] Another retrospective study compared the findings of FDG-PET and MRI in 40 patients with non-CNS malignancy. The sensitivity and specificity of FDG-PET for detecting brain metastases was shown to be 75% and 83%, respectively.[1] Supplementary F-18 FDG PET in 273 patients undergoing evaluation for suspected malignancy, detected pathological lesions in 6 patients (2%). Only 2 of these were unsuspected after CECT.[7] Whole body including brain F-18 FDG PET in 1,026 patients revealed unsuspected skull or cerebral lesions in only 0.4% of the patients. In fact, it has been reported that when scanning of the brain is incorporated into an imaging protocol for patients with non-CNS malignancies, a change in treatment will occur for even less than 1% of patients.[6] The reasons cited for this poor performance include the small size of metastatic lesions, intrinsic spatial resolution of the detectors and close apposition of lesions to metabolically active grey matter.

Although various studies have disapproved the utility of PET for screening of cerebral metastasis with the current day PET/CT scanners having the advantage of short acquisition times (2

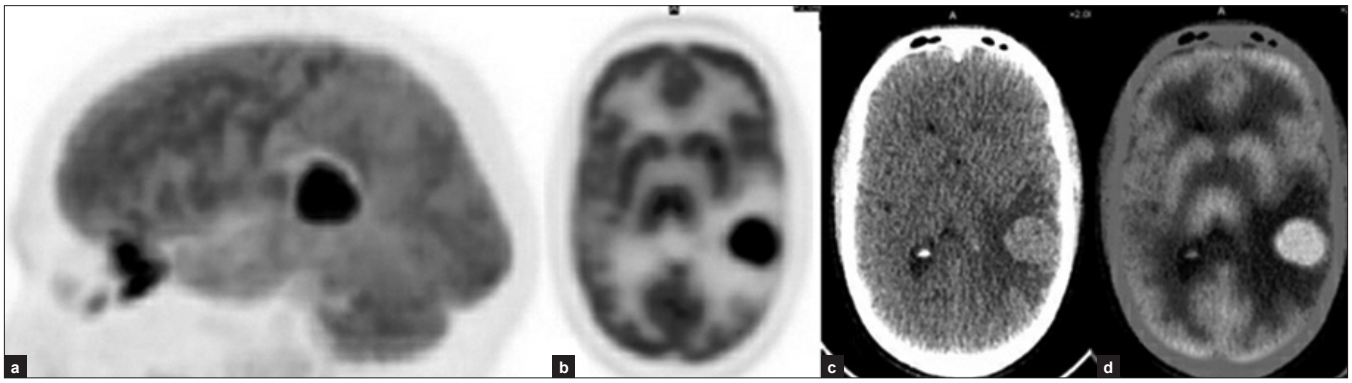

Figure 1: 50-year male with malignant melanoma of the anal canal; (a) Lateral MIP image of the brain shows a hyper-metabolic focus; (b, c, d) Axial plain PET, CT and fused PET/CT images localize the hyper-metabolism to a well-defined hyper-dense lesion in the left parietal region with effacement of atrium of left lateral ventricle with surrounding edema

Table 1: Metabolic characterization of brain lesions detected on PET/CT

Metabolism on PET	Lesions identified	NCCT appearance
Hyper-metabolic	• Metastases (single or multiple), • Epileptogenic zone (ictal or post-ictal) • Acute infarct	• Hyper-dense or iso-dense (associated edema +) • Normal • Hyper-dense
Hypo-metabolic	• Metastases (single or multiple), • Cerebritis, infarcts, gliotic foci, Arachnoid cyst, metastectomy lesion • Radiation necrosis • EPM, CCD	• Hyper-dense or iso-dense (associated edema +) • Hypo-dense • Hyper-dense or iso-dense • Normal

min/bed position) and fused CT for anatomical correlation we strongly feel that the brain must be included in the PET study as it could provide valuable information in these oncology patients (irrespective of the primary). Moreover, in the particular referral subgroup where PET is anyway being done to evaluate extracranial metastatic lesions inclusion of brain can provide valuable timely evidence of intracranial pathology which can further be confirmed by other modalities.

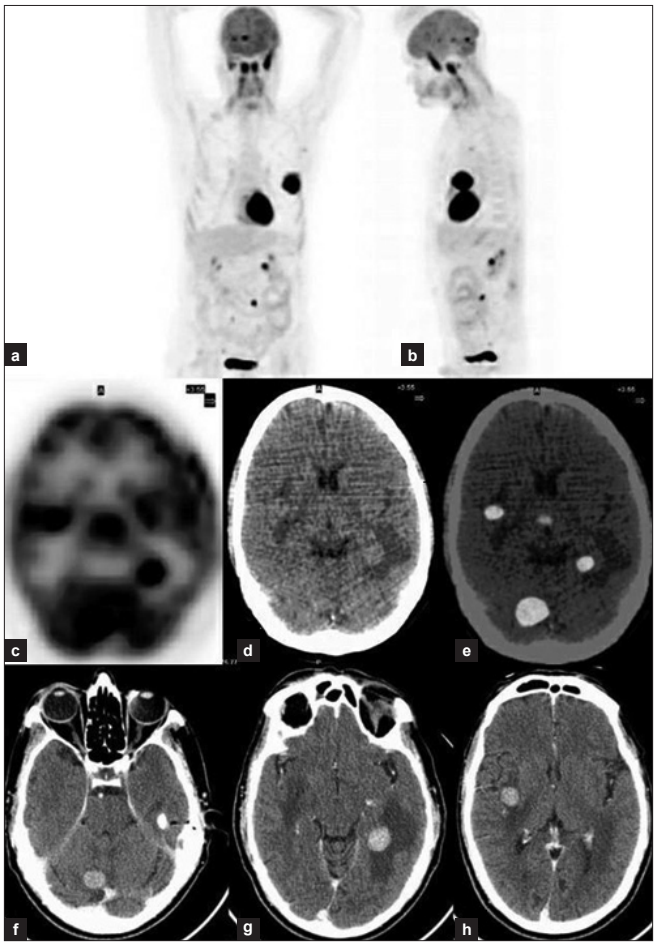

Figure 2: 64-year male Ca left lung for staging; (a, b) Anterior and lateral MIP image showing left lung primary and small hyper-metabolic lesions in the brain; (c, d, e) Axial plain PET, CT and fused PET/CT images localize the foci to the left temporal, right cerebellar and right external capsule region corresponding to mildly hyper-dense lesions on LDCT; (f, g, h) Axial CECT slices clearly depicting the same lesions as intensely enhancing with surrounding edema

Cerebral metastatic lesions can cause seizures in patients. The epileptogenic zone is known to show FDG hyper-metabolism in the ictal phase which may last for up to 48 hours after the seizure. Persistent post-ictal hyper-metabolism in the epileptogenic zone (right parahippocampal gyrus) was seen in a patient with right temporal lobe metastases [Figure 5]. The patient had a seizure in the morning and by the time the PET study was done at least 6 hours had elapsed. The biochemical basis of postictal hyper-metabolism is likely due to energy expenditure for restoration of

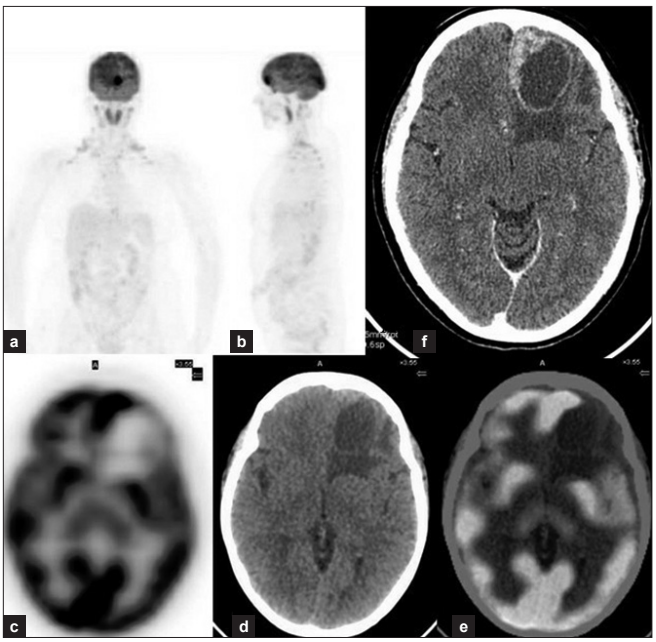

Figure 4: 40-year female, Ca ovary operated three years back, now has rising Ca-125; (a, b) Anterior and lateral MIP image showing a hyper-metabolic foci in the frontal region of the brain; (c, d, e) Axial plain PET, CT and fused PET/CT images reveal FDG accumulation in the left frontal lobe anteromedially corresponding to an iso-dense lesion with edema on CT; (f) Axial CECT shows a peripherally enhancing lesion in the left frontal lobe with a moderately enhancing area in its anteromedial aspect with surrounding edema. Lesionectomy was done and histopathology proved it to be metastatic

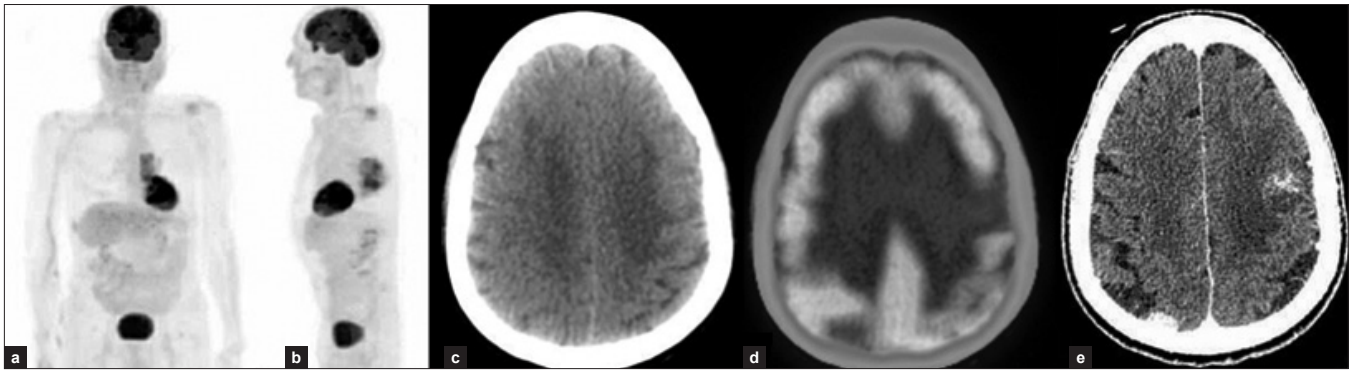

Figure 3: 70-year male papillary adenocarcinoma of the right submandibular gland with bone mets on MRI; (a, b) Anterior and lateral MIP image showing hyper-metabolism in the left lung; (c, d) Axial LDCT and fused PET/CT demonstrate hypometabolism in the left high frontal lobe corresponding to an iso-dense lesion with surrounding edema on CT; (e) Axial CECT at the same level reveals a ring enhancing lesion with surrounding edema in left frontal region and another small homogeneously enhancing lesion in right parietal region

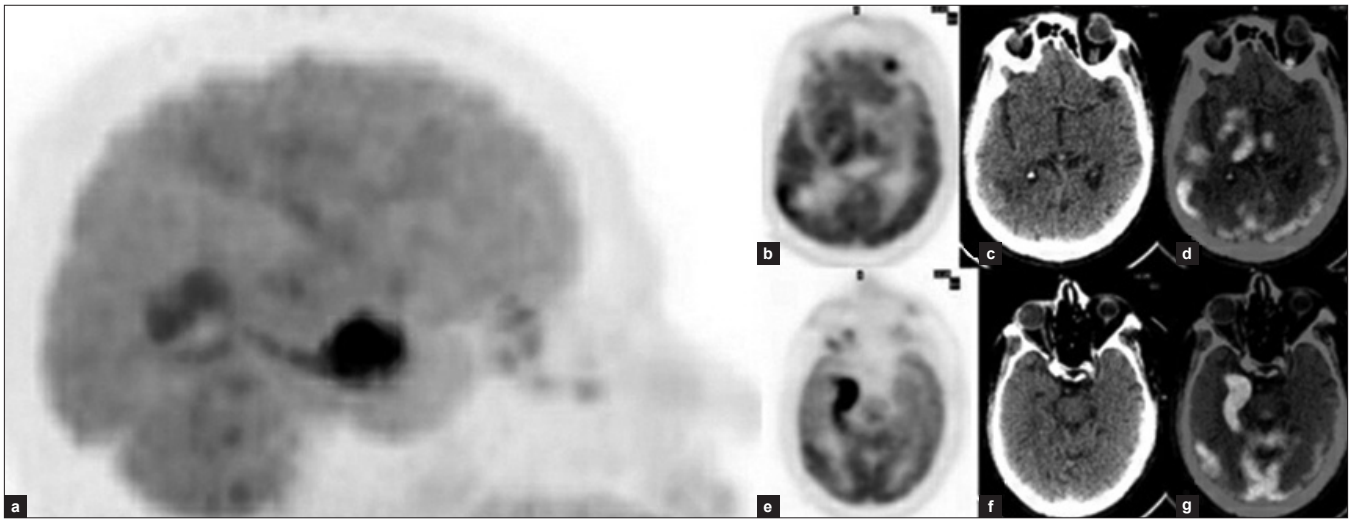

Figure 5: 61-year male with Ca left lung post-chemo/RT with bone mets, sent for evaluation of response to therapy; (a) Lateral MIP of brain showing an intensely hyper-metabolic focus anteriorly and mild hyper-metabolism posterior to it; (b, c, d) Axial plain PET, LDCT and fused PET/CT images localize the posterior hyper-metabolic focus to the right temporo-parietal metastases corresponding to a hyper-dense lesion on NCCT; (e, f, g) Axial plain PET, LDCT and fused PET/CT localize the intensely hyper-metabolic focus to the right parahippocampal gyrus which appears normal on CT

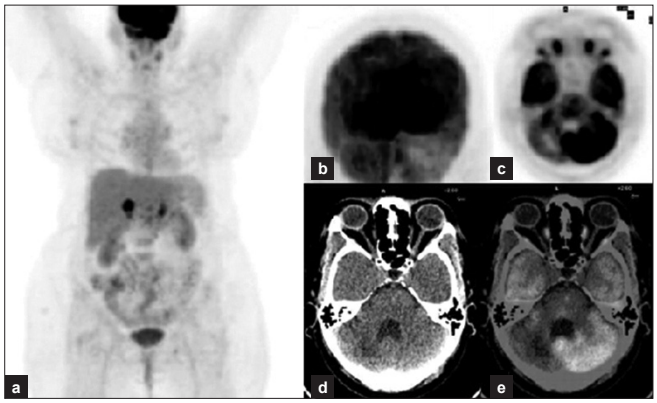

Figure 6: 45-year female Ca breast operated for brain mets undergoing chemo for adrenal mets; (a) Anterior MIP image showing hyper-metabolic foci in both adrenal regions; (b, c, d, e) Posterior MIP of the brain, Axial plain PET, CT and fused PET/CT images reveal hypometabolism in the right cerebellar hemisphere corresponding to a hypodense area on LDCT which corresponded to the site of metastectomy

resting membrane potentials and chemical homeostasis following an epileptic event.[10] Thus, the possibility of hyper-metabolism in epileptogenic zones in patients with cerebral mets must also be kept in mind while reporting the PET study.

Postoperative and postradiation changes

Hypometabolism in areas of successful surgical resection or radiation therapy of metastatic lesions in the brain are evident on the PET study [Figure 6] and can be correlated with patient history, treatment details and the CT findings. Overlying craniotomy defects are visualized in operated patients on NCCT.

Ischemic lesions/ strokes and crossed cerebellar diaschisis

Hypometabolism on PET can also be seen in infarcts which are seen as hypo-dense areas on CT [Figure 7]. Patients usually have a history of an ischemic episode before they were diagnosed with malignancy.

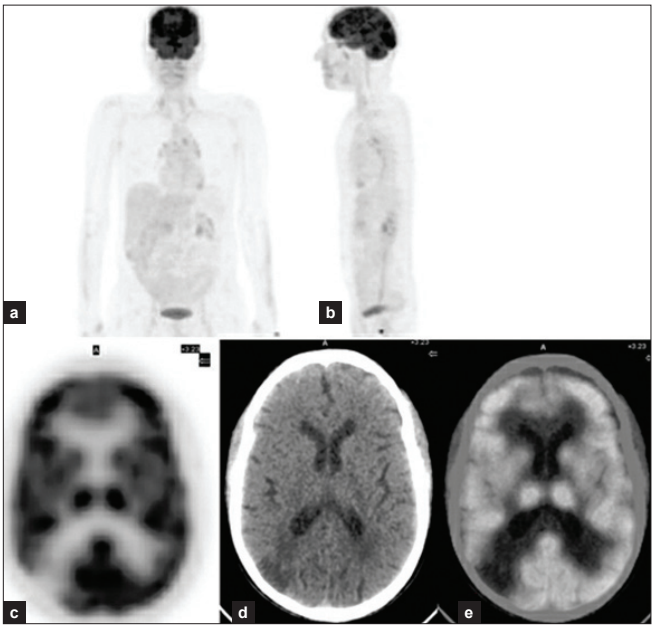

Figure 7: 70-year male case of Ca larynx post-op post-RT on follow-up; (a, b) Anterior and lateral MIP image not remarkable; (c, d, e) Axial plain PET, CT and fused PET/CT images showing hypometabolism corresponding to a well-defined wedge shaped hypodense lesion involving grey and underlying white matter on CT in the right posterior parietal lobe suggestive of a chronic infarct

Strokes can also occur after the diagnosis of cancer and in one study 14% of patients with cancer were found to have cerebrovascular infarction or hemorrhage (CVA) at autopsy. Common causes of CVA in cancer patients include coagulopathy, metastases, therapeutic complications and infection.[11] An acute infarct on the other hand can show increased FDG accumulation [Figure 8] due to inflammation and microglial activation in that region.

The FDG-PET/CT study can also demonstrate crossed cerebellar diaschisis (CCD) in patients with a history of ischemic

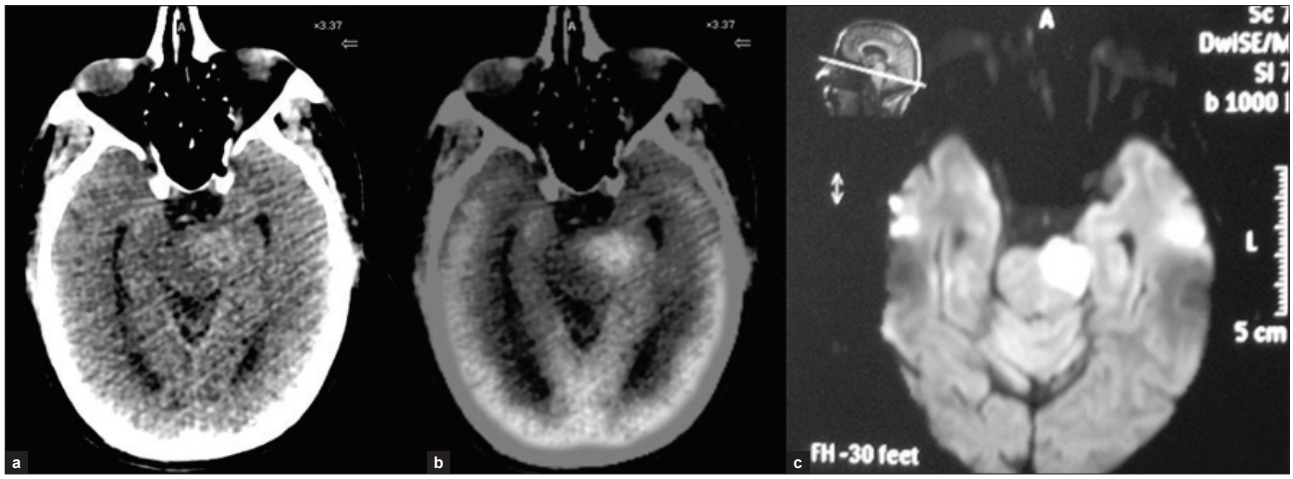

Figure 8: 73-year male Ca lung post CT/RT with history of stroke three weeks back; (a, b) Axial LDCT and fused PET/CT images showing an area of hyper-metabolism corresponding to a hyper-dense lesion in the pons left side; (c) DW MR images show hyper-intense signal and ADC IMAGES showed hypo-intense signal s/o acute infarct

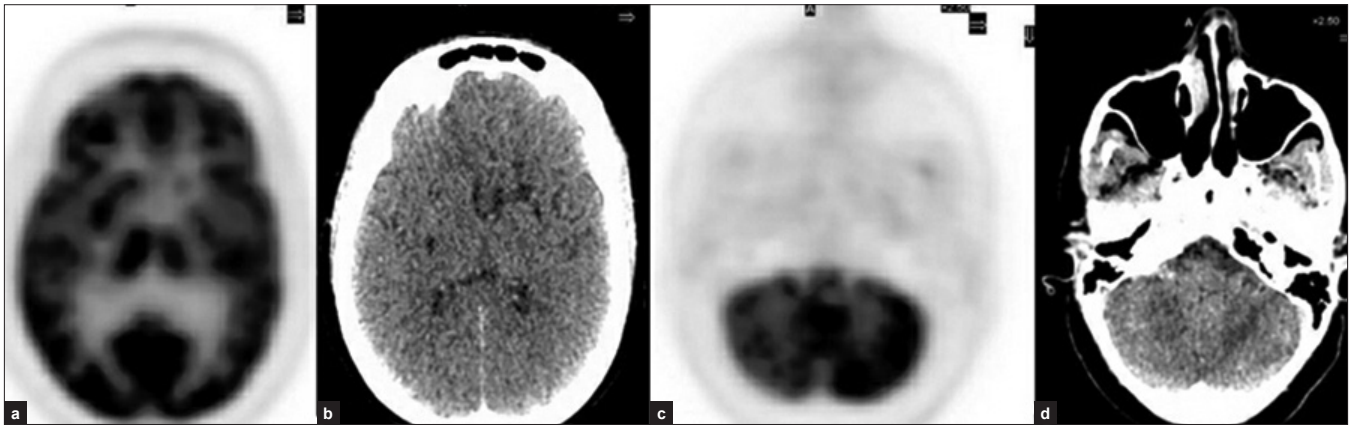

Figure 9: 55-year female Ca right ovary post-op, post-chemo; (a, b) Axial plain PET and CT images showing hypometabolism in the left basal ganglia region corresponding to mild hypo-density on CT in the left MCA territory (infarct); (c, d) Axial plain PET and CT images showing hypometabolism in the entire right cerebellar hemisphere which appears normal on CT consistent with CCD

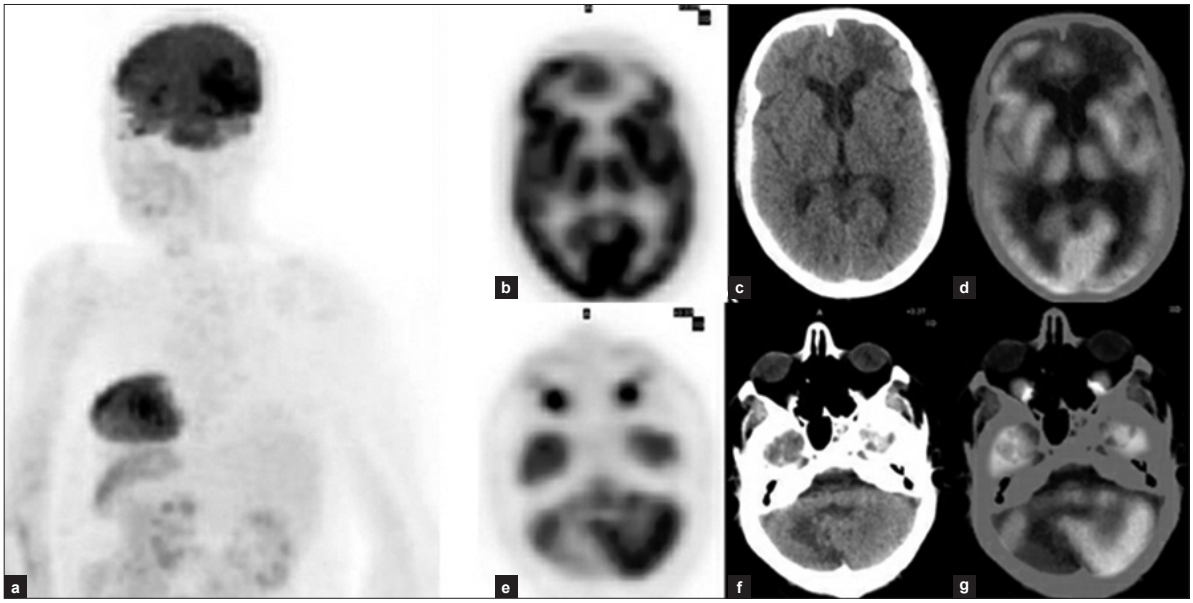

Figure 10: 53-year male treated case of NHL; (a) Right oblique MIP of the brain showing hypometabolism in the cerebellar region; (b, c, d) Axial plain PET, CT and fused PET/CT images show hypometabolism in the left frontal lobe corresponding to a hypo-dense lesion on CT; (e, f, g) Axial plain PET, CT and fused PET/CT images at cerebellar level show hypometabolism in the right cerebellar hemisphere corresponding to a hypo-dense lesion on CT

stroke in a cerebral vessel territory [Figure 9]. This case has been described previously.[12] Interruption of corticopontocerebellar tracts by the infarct causing deafferentation and transneuronal metabolic depression in the contralateral cerebellar hemisphere results in CCD. Interruption of these tracts can occur from a range of injuries including tumor, stroke, gliosis, epilepsy or trauma, with supratentorial ischemic strokes after middle carotid artery occlusion being the most common etiology. It has been demonstrated up to 20 years after a cerebro-vascular accident on FDG-PET.[13]

Traumatic gliosis

Hypometabolism corresponding to hypo-dense lesions involving grey and white matter on CT with dilatation of ipsilateral ventricular horn are suggestive of post-traumatic changes [Figure 10], with or without cortical discontinuity in the overlying calvarium. A detailed history confirms the same.

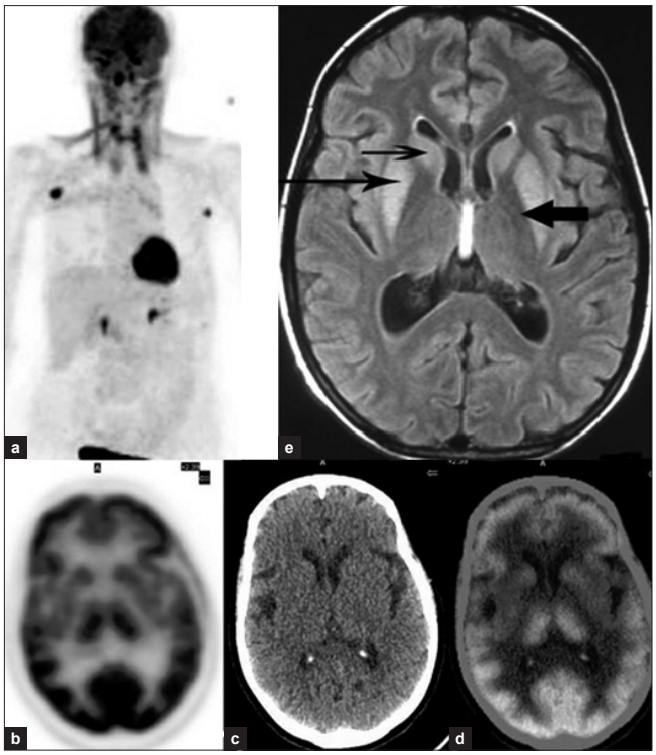

Figure 11: 62-year female treated case of Ca breast on follow up with an episode of hyponatremia which was rapidly corrected; (a) Anterior MIP image showing hyper-metabolic axillary nodes heterogeneity in brain FDG distribution is because patient moved her head during acquisition; (b, c, d) Axial plain PET, CT and fused PET/CT images show hypometabolism in both basal ganglia which appear normal on CT; (e) T2 weighted FLAIR MRI image showing bilaterally symmetrical hyper-intensities in Caudate nucleus and Putamen with sparing of Globus Pallidus suggestive of Extrapontine myelinolysis

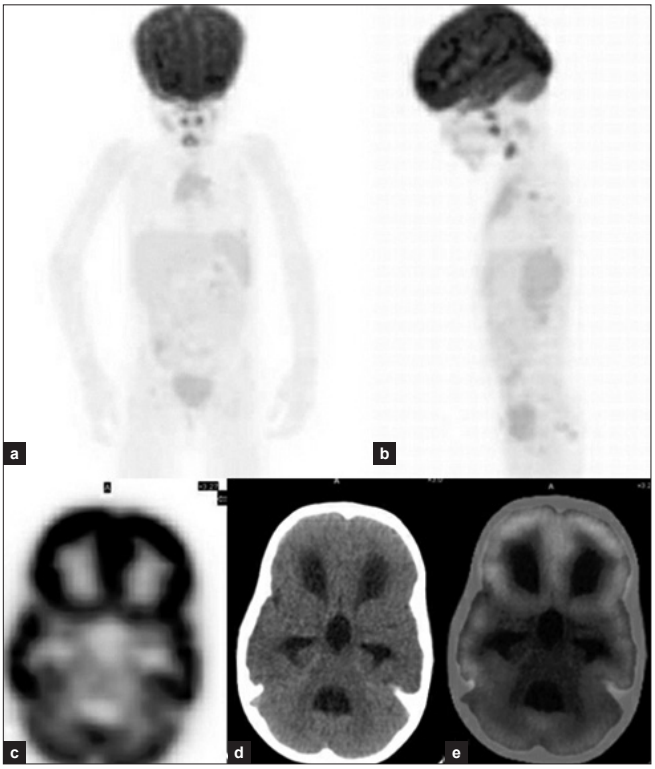

Figure 13: Five-year female of sacrococcygeal teratoma with pulmonary mets sent for evaluation of response to chemotherapy; (a, b) Anterior and lateral MIP; (c, d, e) Axial plain PET, LDCT and fused PET/CT showing moderate communicating hydrocephalus involving B/L lateral, third and fourth ventricles on CT with no FDG metabolism abnormality in the underlying cortex

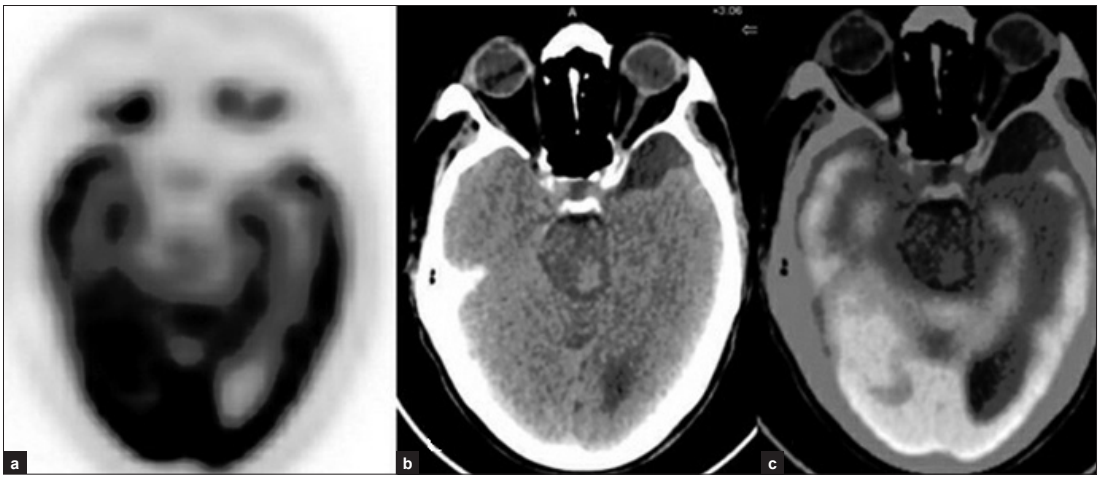

Figure 12: (a, b, c) Axial plain PET, CT and fused PET/CT of a 70-year male Ca lung undergoing evaluation for bone mets shows hypo-dense well marginated extra-axial lesion suggestive of small arachnoid cyst in the left temporal pole on CT with the adjacent part of cortex showing normal FDG distribution

Extrapontine myelinolysis

Myelinolysis is a demyelinating disorder, with relative preservation of blood vessels, neurons and axis cylinders without much inflammation.[14] If it occurs in the region of central basis pontis, it is known as Central Pontine Myelinolysis. In at least 10% of the patients,[15] areas outside the pons are affected, when it is called Extra-Pontine Myelinolysis (EPM). EPM may involve the basal ganglia, thalamus, cerebellum and subcortical white matter with characteristic pallidal sparing[15,16] producing symptoms like tremors, ataxia, decreased speech, oro-bucco-lingual movements.[17] It is basically a hyper-osmotically induced demyelination process[16] and fluctuations in serum sodium levels account for the most well understood underlying mechanism for pathogenesis.[18,19] Even though radiographic signs occur between 7 and 14 days after acute osmotic shift,[14] MRI remains the imaging modality of choice. Typically, T2-weighted and FLAIR MRI images [Figure 11e] demonstrate in increased signal intensity where demyelination has occurred.[15,20] F-18 FDG-PET in EPM has demonstrated initial hyper-metabolism hypothesized to be due to increased glucose activity of the phagocytic microglial cells and astrocytes followed by a delayed hypometabolism [Figure 11] owing to the destructive demyelination[21] as seen in our case.

Arachnoid cyst

Arachnoid cysts are congenital abnormalities most commonly found in the middle cranial fossa and posterior cranial fossa. They are mostly clinically silent. CECT shows an arachnoid cyst as a CSF density mass with slight distortion of adjacent brain structures without peripheral contrast enhancement. It thus comes into the differential diagnosis of hypo-metabolic-hypo-dense lesions on PET/CT [Figure 12].

Hydrocephalus

Hydrocephalus results from an imbalance of production and resorption of CSF in the ventricular system. This imbalance can be congenital or secondary to bacterial or viral CNS infection, hemorrhage or tumor. Ex vacuo ventriculomegaly due to parenchymal brain atrophy associated with aging can also be seen. On CT hydrocephalus is characterized by ventricular enlargement out of proportion to the cerebral sulci widening. On PET, the prominent CSF spaces are visualized as large areas of photopenia surrounded by normal FDG activity in the surrounding compressed grey matter and these findings are well appreciated on fused PET/CT images [Figure 13].

CONCLUSION

Hyper-metabolic lesions are well-identified on the MIP image itself and a fused PET/CT allows further localization of the metabolic abnormality to a structural lesion. Hypo-metabolic lesions if large can be appreciated on the MIP image however the fused PET/CT image helps in structural delineation of the hypo-metabolic lesion and with history correlation an accurate identification of lesion can be obtained. Thus, knowledge of the PET/CT appearance of various brain abnormalities can yield diagnostically relevant information in cancer patients.

REFERENCES

1. Rohren EM, Provenzale JM, Barboriak DP, Coleman RE. Screening for cerebral metastases with FDG PET in patients undergoing whole-body staging of non-central nervous system malignancy. Radiology 2003;226:181-7.
2. Kim YS, Kondzielka D, Flicklligar JC, Lunsford LD. Stereotactic radiosurgery for patients with non-small cell lung cancer metastatic to the brain. Cancer 1997;80:2075-83.
3. Young RF. Radiosurgery for the treatment of brain metastases. Semin Surg Oncol 1998;14:70-8.
4. Nussbaum ES, Djalilian HR, Cho KH, Hall WA. Brain metastases: Histology, multiplicity, surgery and survival. Cancer 1996;78:1781-8.
5. Liu Y. Metastatic brain lesions may demonstrate photopenia on FDG-PET. Clin Nucl Med 2008;33:255-7.
6. Ludwig V, Komori T, Kolb D, Martin WH, Sandler MP, Delbeke D. Cerebral lesions incidentally detected on 2-deoxy-2-[F18]fluoro-D-glucose positron emission tomography images of patients evaluated for body malignancies. Mol Imag Biol 2002;4:359-62.
7. Larcos G, Maisey MN. FDG-PET screening for cerebral metastases in patients with suspected malignancy. Nucl Med Comm 1996;17:197-8.
8. Posther KE, McCall LM, Harpole DH, Reed CE, Putnam JB, Rusch VW, *et al.* Yield of brain F-18 FDG PET in evaluating patients with potentially operable non-small cell lung cancer. J Nucl Med 2006;47:1607-11.
9. Griffeth LK, Keith MR, Dehdashti F, Simpson JR, Fusselman MJ, Guire AH, *et al.* Bain metastases from non-central nervous system tumors: Evaluation with PET. Radiology. 1993;186:37-44.
10. Chugani HT, Shewman DA, Khanna S, Phelps ME. Persistant post-ictal hyper-metabolism. Pediatr Neurol 1993;9:10-5.
11. Rogers LR. Cerebrovascular complications in cancer patients. Neurol Clin 2003;21:167-92.
12. Garg G, Tripathi M, D'Souza M, Sharma R. Crossed cerebellar diaschisis: Demonstrated on F-18 FDG PET/CT. Hell J Nucl Med 2009;12:171-2.
13. Shih WJ, Huang WS, Milan PP. F-18 FDG PET demonstrates crossed cerebellar diaschisis 20 years after stroke. Clin Nucl Med 2006;31:259-61.
14. Chu K, Kang D, Ko SB, Kim M. Diffusion-weighted MR findings of central pontine and extrapontine myelinolysis. Acta Neurol Scand 2001;104:385-8.
15. Bekiesińska-Figatowska M, Bulski T, Rózyczka I, Furmanek M, Walecki J. MR imaging of seven presumed cases of central pontine and extrapontine myelinolysis. Acta Neurobiol Exp (Wars) 2001;61:141-4.
16. Kumar S, Fowler M, Gonzalez-Toledo E, Jaffe SL. Central pontine myelinolysis: An update. Neurol Res 2006;28:360-6.
17. Seiser A, Schwarz S, Aichinger-Steiner M, Funk G, Schnider P, Brainin M. Parkinsonism and dystonia in central pontine and extrapontine myelinolysis. J Neurol Neurosurg Psychiatry 1998;65:119-21.
18. Lampl C, Yazdi K. Central pontine myelinolysis. Eur Neurol 2002;47:3-10.
19. Hsieh CY, Huang CW. Extrapontine myelinolysis in a patient following correction of hyponatremia. Acta Neurol Taiwan 2007;16:188-9.
20. Sepe V. Severe hyponatremia followed by extrapontine myelinolysis. Kidney Int 2006;69:423.
21. Roh JK, Nam H, Lee MC. A case of central pontine and extrapontine myelinolysis with early metabolism of F18DG-PET scan. J Korean Med Sci 1998;13:99-102.

How to cite this article: Tripathi M, Jaimini A, D'Souza MM, Sharma R, Jain J, Garg G, *et al.* Spectrum of brain abnormalities detected on whole body F-18 FDG PET/CT in patients undergoing evaluation for non-CNS malignancies. Indian J Nucl Med 2011;26:123-9.

Source of Support: Nil. **Conflict of Interest:** None declared.